Metallomics, 15, 2023, mfad004
https://doi.org/10.1093/mtomcs/mfad004
Advance access publication date: 20 January 2023
Paper

Depletion assisted hemin affinity (DAsHA) proteomics reveals an expanded landscape of heme-binding proteins in the human proteome

Hyojung Kim [1], Courtney M. Moore [1], Santi Mestre-Fos [1], David A. Hanna [1], Loren Dean Williams [1], Amit R. Reddi [1,*] and Matthew P. Torres [1,2,*]

[1]School of Chemistry and Biochemistry, Georgia Institute of Technology, Atlanta, GA 30332, USA and [2]School of Biological Sciences, Georgia Institute of Technology, Atlanta, GA 30332, USA
*__Correspondence:__ Amit R. Reddi, School of Chemistry and Biochemistry, Georgia Institute of Technology, 950 Atlantic Dr. Atlanta, GA 30033. E-mail: amit.reddi@chemistry.gatech.edu. Matthew P. Torres, School of Biological Sciences, Georgia Institute of Technology, 950 Atlantic Dr. Atlanta, GA 30033. E-mail: mtorres35@gatech.edu.

Abstract

Heme *b* (iron protoporphyrin IX) plays important roles in biology as a metallocofactor and signaling molecule. However, the targets of heme signaling and the network of proteins that mediate the exchange of heme from sites of synthesis or uptake to heme dependent or regulated proteins are poorly understood. Herein, we describe a quantitative mass spectrometry (MS)-based chemoproteomics strategy to identify exchange labile hemoproteins in human embryonic kidney HEK293 cells that may be relevant to heme signaling and trafficking. The strategy involves depleting endogenous heme with the heme biosynthetic inhibitor succinylacetone (SA), leaving putative heme-binding proteins in their *apo*-state, followed by the capture of those proteins using hemin–agarose resin, and finally elution and identification by MS. By identifying only those proteins that interact with high specificity to hemin–agarose relative to control beaded agarose in an SA-dependent manner, we have expanded the number of proteins and ontologies that may be involved in binding and buffering labile heme or are targets of heme signaling. Notably, these include proteins involved in chromatin remodeling, DNA damage response, RNA splicing, cytoskeletal organization, and vesicular trafficking, many of which have been associated with heme through complementary studies published recently. Taken together, these results provide support for the emerging role of heme in an expanded set of cellular processes from genome integrity to protein trafficking and beyond.

Keywords: proteomics, heme, labile heme, heme trafficking, heme signaling, hemoproteomics

Graphical abstract

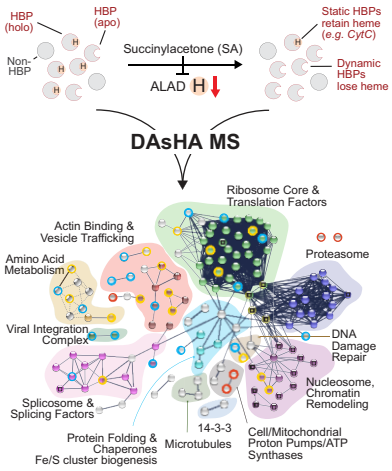

Depletion assisted heme affinity (DAsHA) proteomics reveals an expanded landscape of heme binding proteins.

Introduction

Heme *b* (iron protoporphyrin IX), hereafter referred to as heme, is an essential cofactor and signaling molecule.[1–9] As a cofactor, heme facilitates diverse processes spanning electron transfer, chemical catalysis, and gas binding and transport.[5] As a signaling molecule, heme can bind and regulate the activity and/or expression of a handful of transcription factors,[1,10–15] kinases,[16–19] cell

Received: August 26, 2022. **Accepted:** January 19, 2023

surface receptors,[20] and ion channels.[21–23] Given that heme is also potentially cytotoxic, cells must tightly regulate its concentration and bioavailability.[24–26] The factors regulating the intracellular concentration of heme are well understood, including the mechanisms and atomic resolution structures of all eight heme biosynthetic enzymes and heme degrading heme oxygenases (HO), HO-1 and HO-2.[6–9] However, the molecules and mechanisms that regulate heme bioavailability are comparatively less well understood.

A useful framework for understanding the availability and mobilization of heme in trafficking and signaling is to conceptually partition total cellular heme between exchange inert and labile heme (LH)-binding sites.[8,27–29] Inert heme cannot readily exchange and typically associates with high affinity, buried binding sites, e.g. in cytochromes and globins. Labile heme (LH) can exchange on time scales relevant for physiological heme trafficking, signaling, and buffering. The speciation of LH, including the proteins that bind it, and the targets of heme signaling to which LH may be mobilized, are largely unknown.

There are numerous analytical methods to measure total heme in cell and tissue samples, including HPLC, mass spectrometry (MS), UV/vis spectrophotometry, or indirectly via fluorescence spectroscopy of de-metallated heme, protoporphyrin IX.[8,30] Moreover, identification of high affinity exchange inert hemoproteins can be made on the basis of heme co-purifying with the protein when isolated from native or heterologous sources. However, it is exceedingly challenging to identify proteins that constitute the LH pool and targets of heme signaling using traditional biochemical methods due to facile heme exchange and dissociation upon cell or tissue lysis.

To better understand LH, we and others have developed fluorescence and activity-based heme reporters that can bind exchangeable cellular heme.[27,29,31–35] When coupled with gene deletion or overexpression screens, or screens for drugs, toxins, or various growth conditions and environmental stressors, these heme sensors can reveal new genes and pathways that control LH and heme bioavailability in cells and subcellular compartments. Indeed, by coupling the heme sensors with various genetic, drug, stress, and toxin screens, we previously identified key proteins, e.g. glyceraldehyde phosphate dehydrogenase (GAPDH)[29,36] and GTPases that regulate mitochondrial dynamics and mitochondrial-ER contact sites,[37] nucleic acids, e.g. ribosomal RNA (rRNA) guanine quadruplexes (G4s),[38] small molecules, e.g. nitric oxide (NO),[29] and heavy metal stress, e.g. lead,[39] as factors that regulate or alter LH and heme availability.

Previous studies have reported the heme-binding competent portion of the proteome in a variety of organisms, including humans.[40–42] Most of these studies rely on the enrichment of proteins that bind to hemin–agarose. However, hemin–agarose cannot enrich heme-binding proteins (HBPs) whose heme-binding sites are otherwise occupied by heme, thereby reducing the sensitivity of hemin affinity-MS strategies. Moreover, it is well established that many proteins interact with hemin–agarose despite not being *bona fide* heme dependent or regulated proteins or heme homeostatic factors.[9] Due to these limitations, we hypothesized that the comprehensive hemoproteome has yet to be fully discovered.

Herein, we developed a SILAC (stable isotope labeling with amino acids in cell culture) MS-based proteomics strategy to identify physiologically relevant exchange LH-binding proteins that could contribute to buffering cellular heme or that could act as sources or targets of heme signaling. To distinguish physiological from non-physiological hemin–agarose binding, we devised a strategy that involves first depleting LH with the heme synthesis inhibitor succinylacetone (SA), then identifying proteins that interact specifically with hemin–agarose. The method detects SA-dependent protein interactions with hemin–agarose. In total, the approach reported herein represents the first study of its kind to comprehensively identify the LH proteome in a human cell line without the typical confounding factors associated with heme affinity chromatography (HAC).

Materials and methods

SILAC cell culture

Human embryonic kidney HEK293 cells were obtained from the laboratory of Loren D. Williams (Georgia Institute of Technology). HEK293 cells were cultured for six cell passages in SILAC media consisting of Powdered DMEM Medium for SILAC (Thermo, #88425), L-leucine (105 mg/l, Sigma, #L8912), L-proline (200 mg/l, Sigma #L5607), 2% penicillin-streptomycin (VWR, #97063-708), and 10% Dialyzed Fetal Bovine Serum (R&D Systems, #S12850) supplemented with either 0.798 mM 'heavy' L-lysine-13C6, 15N2 (Lys8, Cambridge Isotope Laboratories, #CNLM-291-H) or 0.398 mM 'heavy' L-arginine-13C6, 15N4 (Arg10, Cambridge Isotope Laboratories, #CNLM-539-H) for SILAC heavy group or the same concentrations of 'light' L-lysine (Lys0, Sigma, #L8662), and L-arginine (Arg0, Sigma, #A6969) for SILAC light group at 37°C in 5% CO_2.

SA treatment and cell lysis

One pair of SILAC 'light' and 'heavy' groups were treated with 500 μM SA for 48 h (SA+), and the other pair were treated with DI water (SA−) with three biological replicates. The SILAC-labeled HEK293 cells with or without SA were harvested in 1X PBS and lysed by three cycles of the freeze (−80°C)-thaw method in 10 mM phosphate buffer pH 7.4 with 50 mM NaCl, 5 mM EDTA (G-Biosciences, #015E-F), 1X ProteaseArrestTM (G-Biosciences, #71003-168), 1 mM PMSF (G-Biosciences, #786), and 0.1% Triton X-100 (AMRESCO, #0694).

Heme affinity chromatography

To perform HAC, 1.5 mg protein lysate was incubated with 150 μl bead bed of pre-equilibrated hemin–agarose (Sigma, #H6390) for SILAC 'heavy' group and the same bead bed volume of pre-equilibrated Sepharose (Sigma, #4B200) in HAC buffer (10 mM phosphate buffer pH 7.4 with 50 mM NaCl, 5 mM EDTA, 1X ProteaseArrestTM, and 1 mM PMSF) for 1 h at 20 rpm at a rotator at room temperature. The incubated beads were washed three times with HAC buffer and eluted in 1 M imidazole (Sigma, #IX0005) in HAC buffer.

Total heme measurements

Measurements of total heme were accomplished using a fluorometric assay designed to measure the fluorescence of protoporphyrin IX upon the release of iron from heme, as previously described.[43] After harvesting HEK293 cells, the cells were counted using an automated TC20 cell counter (BioRad). At least 500 000 cells were resuspended in 400 μl of 20 mM oxalic acid overnight at 4°C protected from light. After the overnight incubation, an equal volume of 2 M warm oxalic acid was added to give a final oxalic acid concentration of 1 M. The oxalic acid cell suspensions were split, with half the cell suspension transferred to a heat block set at 100°C and heated for 30 min and the other half of the cell suspension kept at room temperature (25°C) for 30 min. All suspensions were centrifuged for 3 min on a table-top microfuge at 21 000 g, and the porphyrin fluorescence (ex: 400 nm and em: 620 nm) of 200 μl of each sample was recorded on a Synergy Mx

multi-modal plate reader using black Greiner Bio-One flat bottom fluorescence plates. Heme concentrations were calculated from a standard curve prepared by diluting 2.5–200 nM hemin chloride stock solutions in 0.1 M NaOH into oxalic acid solutions prepared the same way as for the cell samples. To calculate heme concentration, the fluorescence of the unboiled sample (taken to be the background level of protoporphyrin IX) is subtracted from the fluorescence of the boiled sample (taken to be the free porphyrin generated upon the release of heme iron). The cellular concentration of heme is determined by dividing the moles of heme determined in this fluorescence assay and dividing by the number of cells analyzed, giving moles of heme per cell, and then converting to a cellular concentration by dividing by the volume of a HEK293 cell, assumed to be 1.2 pl.[44]

LH measurements

LH was measured using a previously reported genetically encoded heme sensor, HS1.[29,37–39,43,45,46] HS1 was expressed using the pcDNA3.1 plasmid and driven by the CMV promoter, as previously described.[38,43] For heme sensor transfections, 1/24 of the HEK293 cells from a confluent T75 flask were used to seed 2 ml of cultures in each well of polystyrene-coated sterile six-well plates (Greiner). Once the cells were 30–50% confluent, typically 1–2 days after seeding, the media was changed to 2 ml of fresh regular media (DMEM), with 4.5 g/l glucose and without L-glutamine and sodium pyruvate, supplemented with 10% v/v FBS (heat inactivated) 60 min before transfection. For each well to be transfected, 100 μl of a plasmid transfection master mix was added. The master mix was prepared by mixing, in order: 600 μl OptiMEM (100 μl per well up to 600 μl), 2 μg of heme sensor plasmid, a volume of Lipofectamine Plus Reagent equal in μl to the μg of plasmid DNA used, and a volume of Lipofectamine LTX transfection reagent that is double the volume of the Lipofectamine Plus Reagent. Before adding the transfection mixture to each six-well plate, the master mix was mixed by gentle pipetting and allowed to incubate at room temperature (25°C) for 5 min. Forty-eight hours after transfection, the media was changed to fresh regular media, regular media with 500 μM SA, regular media with 350 μM aminolevulinic acid (5-ALA), or heme deficient and SA (HD + SA) treated media. HD media was prepared by using heme-depleted FBS, which was produced by incubating it with 10 mM ascorbic acid at 37°C in a shaking incubator at 200 RPM for 8 h.[16,43] Loss of heme was monitored by measuring the decrease in Soret band absorbance at 405 nm. Eighty milliliter of ascorbate-treated FBS was then dialyzed against 3 l of PBS, pH 7.4, three times for 24 h each at 4°C, using a 2000 MWCO membrane (Spectra/Por 132625). Dialyzed FBS was then filtered and sterilized with a 0.2 μm polyethersulfone filter (VWR 28145-501) and syringe (VWR 53548-010). The cells were then cultured for an additional 48 h before harvesting for flow cytometric analysis of sensor fluorescence.

For flow cytometric analysis of sensor fluorescence, the cells were washed and resuspended in 1 ml of PBS, transferred to a 1.5 ml microfuge tube, and pelleted at 400 g and 4°C for 4 min. The supernatant was decanted, and the cells were resuspended in 500 μl PBS. The cell suspensions were filtered through a 35 μm nylon filter cap on 12 × 75 mm round bottom tubes (VWR/Falcon 21008-948). Flow cytometric measurements were performed using a BD LSR Fortessa, a BD LSR II, or a BD FACS Aria Illu flow cytometer equipped with an argon laser (ex: 488 nm) and a yellow–green laser (ex: 561 nm). Enhanced green fluorescent protein was excited using the argon laser and was measured using a 530/30 nm bandpass filter, whereas mKATE2 was excited using the yellow–green laser and was measured using a 610/20 nm bandpass filter. Data evaluation was conducted using FlowJo v10.4.2 software. Single cells were gated by size (FSC versus SSC), and only mKATE2 positive cells that had median mKATE2 fluorescence were selected for ratiometric analysis, which typically corresponded to ∼5000 cells.

HS1 sensor heme occupancy was determined according to Equation (1).[29,43]

$$\%\ \text{Heme Occupancy} = \frac{R - R_{\text{max}}}{R_{\text{max}} - R_{\text{min}}} \times 100.$$

R_{min} and R_{max}, the median eGFP/mKATE2 sensor fluorescence ratios when the sensor is depleted of or saturated with heme, respectively, were determined from cultures grown in HD + SA media or media supplemented with 5-ALA. 'R' is the median sensor ratio in regular media or regular media supplemented with SA.

Trypsin digestion

The eluates of SILAC 'heavy' and 'light' were combined for each SA+ and SA− group, respectively, followed by reduction in 5 mM TCEP (VWR, #97064-848) for 1 h and alkylation in 10 mM iodoacetamide (VWR, #97064-926) in dark for 30 min. Protein pellet of each SA+ and SA− group was obtained by removing the aqueous and organic layers consecutively following the addition of 4 volumes of methanol (Sigma, #34860), 1 volume of chloroform (ACROS Organics, #423550250), and 3 volumes of water (Sigma, #270733) and centrifugation at 4°C at 21 000 × g for 10 min. The protein pellets were resuspended in 100 mM Tris-HCl pH 8, 1 M ammonium bicarbonate, 6 M urea followed by incubation for 1 h at 37°C, and dilution of the urea down to 1.5 M with LC-MS grade water. The resuspended protein samples were enzymatically digested by trypsin with 1:20 (w/w) of enzyme to substrate ratio at 37°C overnight.

High-pH RPLC fractionation for whole proteome

The SILAC-labeled peptides were pre-fractionated by high-pH reverse phase liquid chromatography using an Agilent 1100 HPLC system with Waters XBridge C18 reverse phase column (4.6 × 250 mm, 3.5 μM, 130 Å) with 10 mM ammonium formate (solvent A, Fluka, #17843) and 10 mM ammonium formate in 90% acetonitrile (solvent B, EMD Millipore, #AX0145) adjusted to pH 10 using ammonium solution (EMD Millipore, #105426). Fractions were collected every 1 min at a flow rate of 700 μl/min using a gradient method (from 0 to 75% solvent B in 60 min). The collected fractions were frozen at −80°C followed by CentriVap lyophilization.

LC-MS/MS analysis

Peptide fractions were analyzed by LC-MS/MS using a Q Exactive Plus orbitrap mass spectrometer equipped with an UltiMate 3000 LC system (Thermo). The lyophilized fractions were resuspended in 0.1% formic acid (FA) in 5% acetonitrile (ACN) and loaded onto NanoViper trap column (75 μm ID × 20 mm) packed with AcclaimTM PepMap 100 C18 (3 μm, 100 Å). The samples were resolved through a NanoViper analytical column (75 μm ID × 150 mm) packed with Acclaim PepMap 100 C18 (2 μm, 100 Å) at a flow rate of 0.3 μl/min with solvent A (0.1% FA in 2% ACN) and solvent B (0.1% FA in 90% ACN) for 150 min. Data-dependent tandem MS was conducted with the full scans in the range from 200 to 1800 m/z using an Orbitrap mass analyzer where automatic gain control being set at 3e6 (MS1) and 1e5 (MS2), resolution at 70 000 (MS1) and 17 500 (MS2), and Max IT at 100 ms (MS1) and 50 ms (MS2). The top 15 most abundant precursor ions were selected at MS1 with an isolation window of 4 m/z and further fragmented

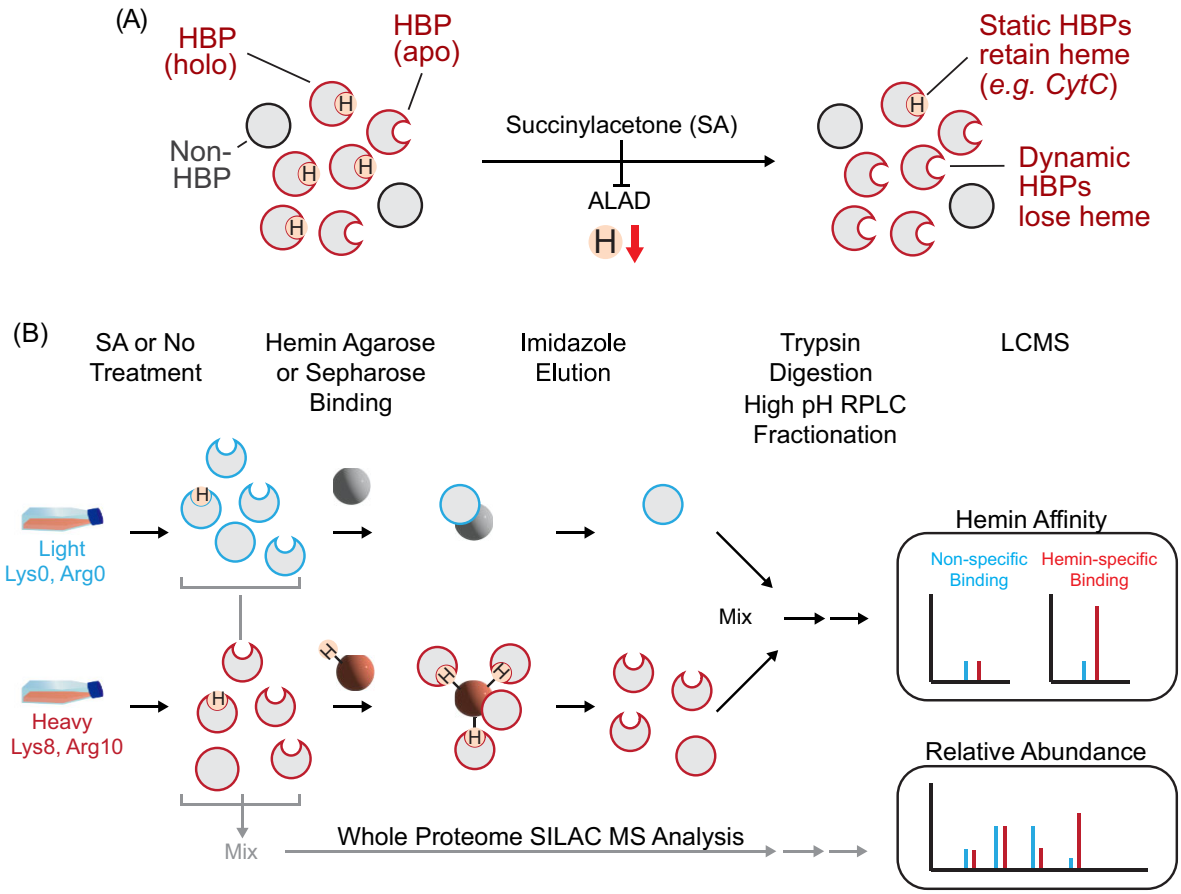

Fig. 1 Schematic diagram of DAsHA MS. (A) SA treatment inhibits ALAD to reduce cellular heme concentrations and increase the frequency of apo-HBPs compared to holo- (heme bound) HBPs. (B) Cells grown in either light or heavy amino acid media are treated with (SA+) or without SA (SA−). The resulting cells are lysed, and a fraction is mixed for direct LCMS analysis of proteome-wide relative protein abundance (light gray arrows). The remainder of the samples is kept unmixed and exposed in equal amounts to equivalent proportions of either hemin–agarose beads (lower path) or beaded sepharose lacking heme (upper path). After binding and elution with imidazole, the entire eluate from each path is mixed, digested with trypsin protease, and fractionated offline followed by LCMS of each fraction. Peptides from proteins binding non-specifically to both bead types have SILAC ratios at or near unity, whereas hemin-specific binding proteins exhibit ratios much greater than unity. HBP = heme binding protein; SA = succinylacetone

at MS2 by high energy collisional dissociation (HCD) with normalized collision energies (NCEs) of 28.

MS data analysis

MS raw data were searched against UniProt Homo sapiens (Human) proteome (UP000005640) using Proteome Discoverer 2.0 with 10 ppm MS precursor mass tolerance, 0.02 Da MS fragment mass tolerance, and 0.01 false discovery rate. SILAC protein ratios ('heavy' hemin–agarose/'light' sepharose for both SA+ and SA− conditions and 'heavy' SA+/'light' SA− for WP) were calculated based on the ratio of integrated peak areas at MS1 for SILAC 'heavy' and 'light' peptides. Statistical significance of specific hemin–agarose binding of proteins based on the SILAC protein ratio ('heavy' hemin–agarose/'light' sepharose) for both SA+ ($n = 3$) and SA− ($n = 3$) were determined, respectively, using response screening in JMP 16.0. Proteins with either 'heavy' or 'light' values only were separately processed and reported as +/− infinite change in specific hemin–agarose binding and protein abundance.

Physical interaction networks and ontology enrichment

Ontology analyses were accomplished using string-db.org version 11.5. Data were filtered for high-confidence interactions and clustered using MCL clustering with inflation parameter 3 (default). In cases where there was significant overlap across multiple terms, ontological terms that provided the greatest coverage with minimal overlap between core groups were identified through manual interrogation and highlighted as described in each figure. Aggregate statistics, further analyses, and quantitative graphics were generated using JMP Pro version 16 (SAS Inc.).

Results

DAsHA proteomics

LH protein complexes can readily exchange heme with other molecules on physiologically meaningful time scales. Such complexes represent sites for buffering excess heme and a source of exchangeable heme for heme dependent or regulated proteins. Hemin–agarose-based HAC is a commonly used method to enrich potential HBPs. However, labile hemoproteins are expected to bind heme at some fractional level reflecting an equilibrium between its heme bound and free states. This fractional saturation reduces the concentration of *apo* HBPs that are competent to bind hemin–agarose and prevents the binding of *holo* HBPs that are already complexed with heme. Theoretically, shifting the equilibrium between *holo* and *apo* HBP states should, therefore, be achievable by depleting cellular heme with SA, an inhibitor of the second

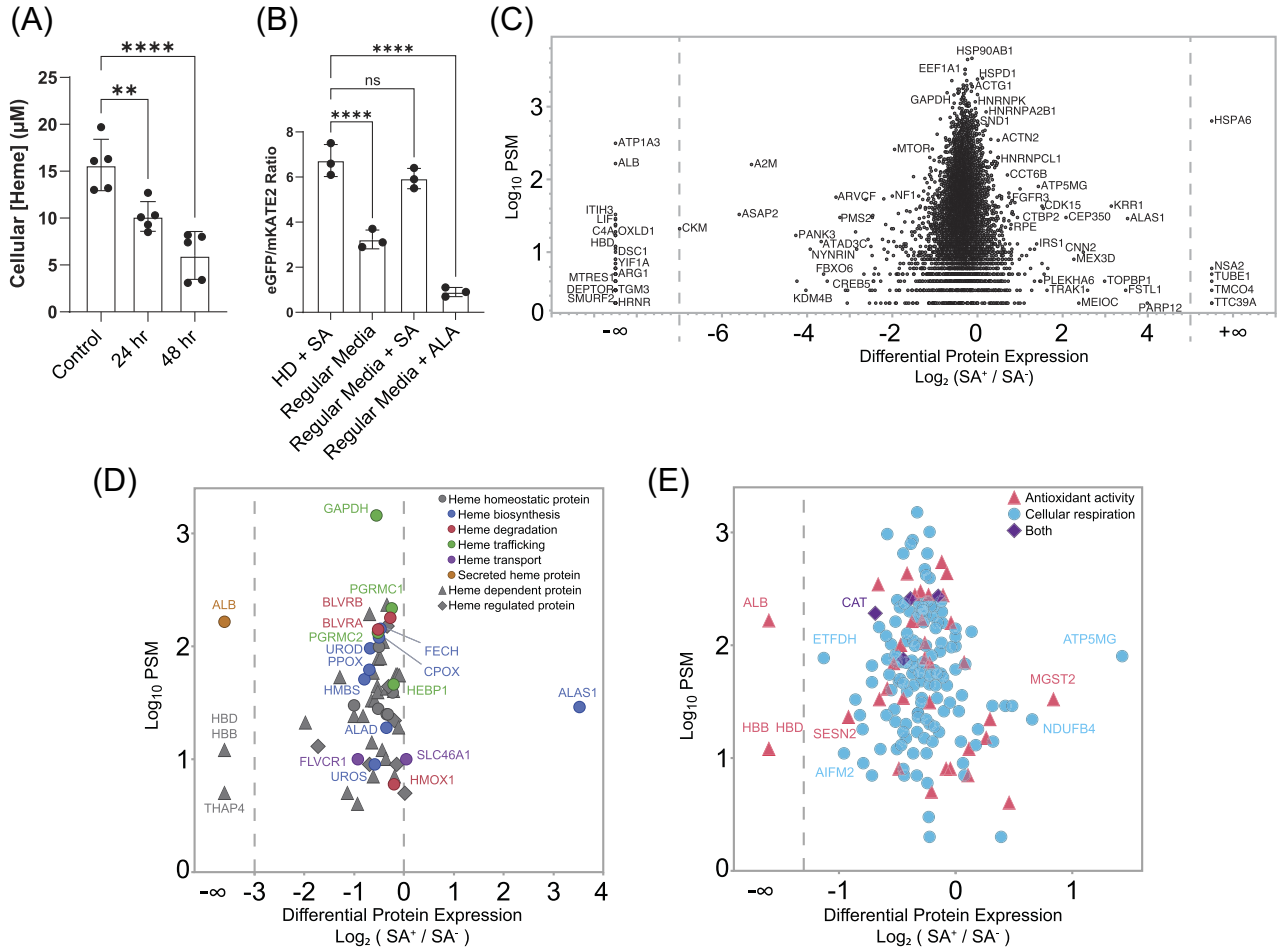

Fig. 2 Heme depletion has a minor effect on most, but not all, proteins in the proteome. (A) Effect of 24- or 48-h SA treatment of HEK293 cells on total intracellular heme concentrations. (B) Effect of 48-h SA treatment of HEK293 cells on LH as measured by the genetically encoded heme sensor HS1. (C) SILAC-MS results for WP measurement of protein differential expression in 48 h SA+ versus SA− conditions. Peptide spectral matches correspond with the sum across all peptides for each protein. Proteins visible in only one of two conditions are shown as +/− infinity on the x-axis. (D, E) Subset of proteins from B enriched in specific GO terms associated with cellular heme. Plots are broken into two parts to reduce crowding. (See also Tables S1 and S2.) Heme homeostatic proteins are defined as those with known effects on heme synthesis, degradation, transport, and trafficking. Heme dependent proteins are those defined as requiring heme for activity. Heme regulated proteins are those that exhibit activities that are modulated by heme but that do not require heme for function.

enzyme in the heme biosynthetic pathway, aminolevulinic acid dehydratase (ALAD) (Fig. 1A and B). We developed a quantitative MS-based hemoproteomics workflow that capitalizes on this idea in order to reveal new HBPs that have yet to be discovered through traditional hemin–agarose enrichment (Fig. 1).

In this method, called DAsHA-MS, cells are grown in the presence or absence of SA, each condition of which is separately grown with light and heavy amino acids (L-lysine and L-arginine) so as to enable quantitative MS of both affinity enrichment specificity and proteomic analysis of SA+/− cells (see materials and methods). In these experiments, light and heavy signals are primarily used to distinguish specific from non-specific binding on hemin–agarose versus beaded sepharose (control), respectively. For example, proteins from light or heavy cells conditioned with SA (SA+) are exposed to equivalent amounts of beaded sepharose or hemin–agarose, respectively. The resulting eluate from both bead types is then mixed 1:1, digested with trypsin, and analyzed by LCMS. Identical processing is carried out in parallel for the SA− condition. The SILAC ratio for each peptide/protein reflects the relative specificity of the detected protein for hemin–agarose over control. In parallel, SA+ (heavy) and SA− (light) proteomic samples are also mixed and analyzed *pre-enrichment* by LC-MS/MS to determine changes in protein abundance that may result from SA treatment (see methods and materials). The resulting data are overlayed to provide cellular abundance context for each protein detected by affinity purification.

Heme depletion has a large effect on a small subset of proteins in the human proteome

We carried out DAsHA analysis for three independent biological replicate samples of HEK293 cells (see methods and materials). Heme depletion was accomplished by treating cells with 500 μM SA for 48 h, which resulted in a 3-fold depletion of total heme (Fig. 2A), in line with prior studies using SA in HEK293 cells, and complete ablation of exchange LH as measured by the genetically encoded fluorescent heme sensor, HS1 (Fig. 2B).[29,38,43,47] Notably, SA-dependent heme depletion did not affect cell viability (Fig. S1A). The eGFP to mKATE2 fluorescence ratio of HS1 is a reporter of LH, with a high ratio indicating low heme and a low ratio indicating high heme. Ratios are calibrated against cells grown under

heme deficient conditions (HD + SA) or heme saturating conditions [media supplemented with the heme biosynthetic intermediate aminolevulinic acid (5-ALA)] (see materials and methods). To establish the effects of this treatment on proteome-wide protein abundance, we carried out whole proteome (WP) SILAC-MS analysis of each sample. At scale, we found that SA treatment has a minor effect on the abundance of most proteins across the entire proteome, with an approximate 20% decrease as determined by SILAC ratios (Fig. 2C, Table S1, and Fig. S1B). This trend was consistent for the established network of known heme-associated proteins within the human proteome, including cellular activities coupled to heme regulation and toxicity and proteins involved in cellular respiration or antioxidant activity (Fig. 2D and E).

A small proportion of proteins undergo extreme changes in abundance in response to SA treatment as indicated by an extremely large SILAC ratio or the lack of signal from one of the two samples (see $+/-\infty$) (Fig. 2C–E and Table S2). We found that in several cases, these proteins either rely on heme binding for stability, such as hemoglobin (HBB) or albumin (ALB).[48] In contrast, we also observed dramatic increases in a small subset of proteins, including the heme biosynthetic enzyme Alas1 (5′-aminolevulinate synthase), which undergoes repressed transcription and accelerated protein degradation in response to heme binding and should therefore increase in response to heme depletion (Fig. 2B).[49] Lastly, we also observed extreme abundance changes in several other proteins not previously known to be heme regulated, which may represent a putative set of heme regulated proteins, albeit not necessarily through direct interaction with heme (Table S3). These include nuclear, cytoplasmic, cell membrane, Golgi, ER, and secreted proteins that may constitute a protein network whose abundance regulation, either through expression or degradation, relies heavily on cellular heme concentrations.

Proteins undergoing extreme abundance changes in response to heme depletion were also highly enriched in phosphoproteins, some of which are linked to immune response, cell export, and endocytic vesicles (Fig. S2). None of these phosphoproteins were detected by DASHA (described below), suggesting that they reflect a stress response to heme depletion with SA, rather than direct targets of heme regulation. Together, these data indicate that SA treatment effectively depletes cellular heme, that such depletion produces expected effects on proteins known to be regulated by heme, but has an overall minor effect on the proteome at large. Furthermore, these data uncover a network of phosphoproteins sensitive to dynamic cellular heme concentrations albeit through mechanisms likely independent of direct heme binding.

Heme depletion boosts the detection of hemin–agarose-binding proteins from the human proteome

In parallel with the WP analysis, samples were subjected to hemin–agarose enrichment to reveal heme-specific binding proteins, wherein specificity is quantified by the ratio of protein binding to hemin–agarose versus control sepharose beads lacking conjugated heme. We observed a total of 343 and 480 proteins enriched >2-fold on hemin–agarose compared to sepharose in the SA− and SA+ conditions, respectively (Fig. 3A, B and Table S4). Overall, non-specific binding to sepharose was low, which we confirmed by SDS-PAGE and Coomassie protein staining (Fig. 3C). After filtering protein IDs by significance ($-\text{Log}_{10}$ P-value >1.3), those proteins identified exclusively upon enrichment with hemin–agarose but not in the sepharose controls were classified as *high* hemin specificity, while proteins identified in both hemin–agarose and sepharose controls ($1 < \text{Log}_2 < 10$) were classified as *moderate* hemin specificity (Table S4). Importantly, despite showing some tendency to bind non-specifically to sepharose, several proteins classified as having moderate specificity were in fact enriched by as much as 70-fold by hemin–agarose compared to sepharose.

To evaluate the effect of heme depletion on protein capture, we first compared the comprehensive list of proteins identified ($\text{Log}_2 \geq 1$) in the SA− versus SA+ conditions, regardless of significance (309 proteins). While the majority of proteins observed between the two conditions overlapped (197 proteins; 64%), we found a large increase in the number of unique proteins identified only after SA treatment (90 proteins; 29%) in contrast to 22 proteins (7%) observed exclusively in the absence of SA treatment (Fig. 3D). Importantly, overlap between protein IDs found in both SA− and SA+ conditions is expected for proteins whose cellular populations are only fractionally saturated with heme. When restricting the comparison to high hemin specificity proteins, we observed 122 proteins in total (SA− and SA+), wherein there was a 30% overlap (37 proteins) between the two conditions and 44 high specificity proteins (36%) in SA+ compared to 41 proteins (34%) in the SA− condition (Fig. 3E). A total of 42 (95%) of the 44 SA+ high specificity proteins were not enriched at all in the SA− condition, regardless of significance and fold change thresholds. In contrast, all but seven proteins in the SA− high specificity class were also detected in the SA+ condition regardless of these same thresholds. Taken together, these data demonstrate that depletion of cellular heme prior to hemin–agarose enrichment has a bulk advantage in boosting the detection of HBPs in the human proteome. Furthermore, these data support the hypothesis that a subset of the human proteome is involved in interacting (directly or indirectly) with the dynamic LH pool in cells.

Validation of MS-identified HBPs visible only after heme depletion

To validate our MS-based results, we conducted an immunoblot analysis of proteins from SA− or SA+ conditioned cells. Samples were again enriched on either sepharose or hemin–agarose beads followed by immunoblotting with antibodies to ATP1A-1/2/3, G3BP1, and PHB. GAPDH, which we and others have previously shown interacts with and traffics LH,[29,36,50–53] was included as a positive control. For each of the three test proteins, strong enrichment was observed with hemin–agarose over sepharose, consistent with their high specificity classification by SILAC MS (Fig. 4). Also consistent was our finding that GAPDH interacts mildly with sepharose, which we also observed by SILAC MS (Table S4). Each protein, including the GAPDH control, showed an increase in hemin–agarose binding in the SA+ condition, which supports the conclusion that heme depletion has a bulk positive effect on boosting enrichment of LH binding proteins. These data provided strong support for the validity of the MS results and suggested that the method captures LH-binding proteins that may not be detected through traditional approaches that do not deplete cellular heme.

Ontology enrichment reveals higher than average physical connectivity for HBPs

To gain insight into the human proteomic targets of heme, we conducted ontological enrichment of the comprehensive list of proteins (moderate or high specificity) observed in both SA− and SA+ conditions with significance ($P < 0.05$). Of this list of 218 proteins, 213 matched to a protein in the STRING ontology database. Generally speaking, these proteins show significant enrichment across

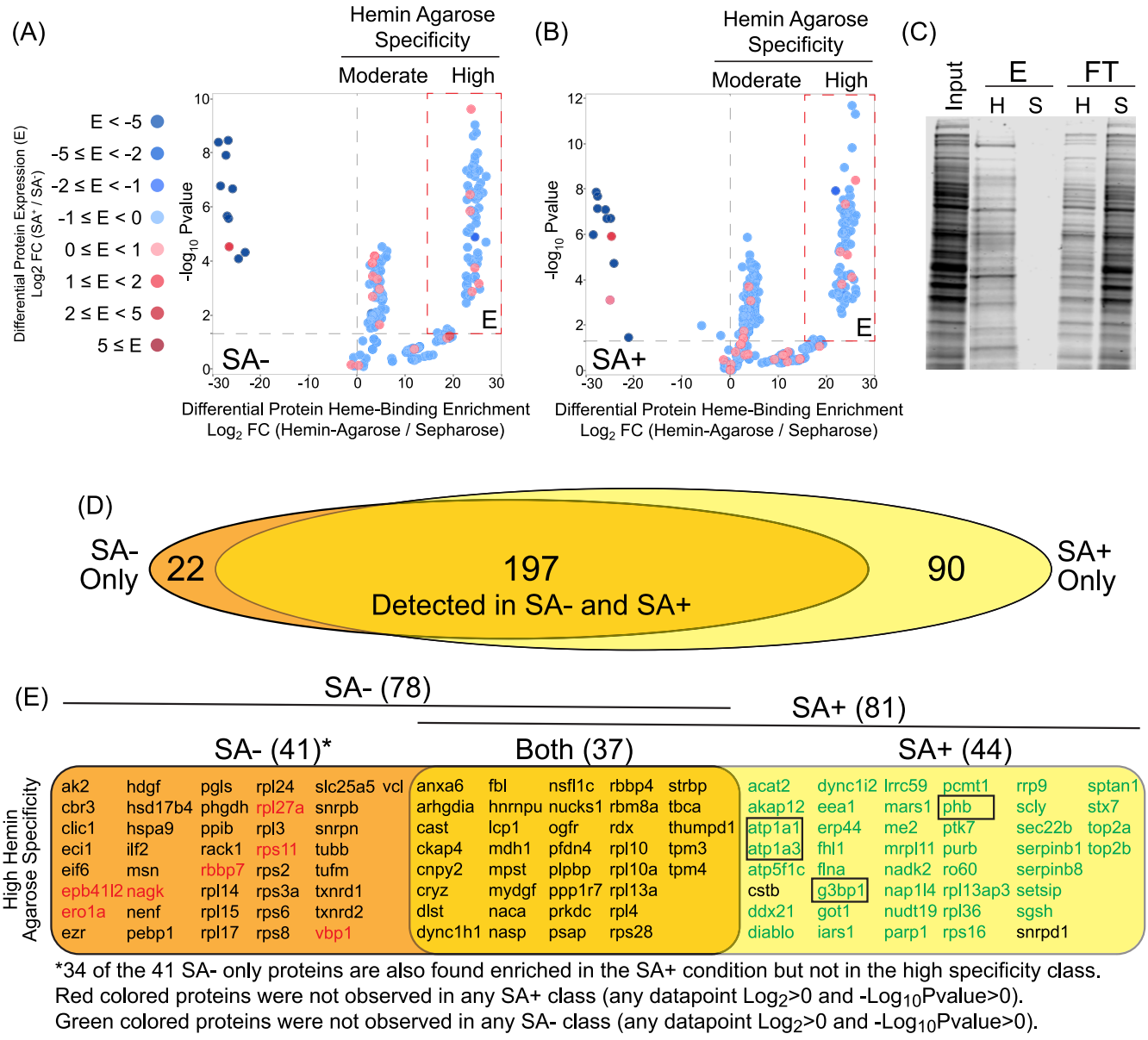

Fig. 3 Heme depletion increases the detection of LH-binding proteins. (A-B) Plot of hemin–agarose-specific binding proteins in the SA (A) and SA+ (B) conditions. The Log2 SILAC ratio for each protein in the hemin–agarose versus the sepharose control. Proteins are clustered into 'moderate' and 'high' specificity classes, where high specificity proteins are those that were detected only in the presence of hemin–agarose. Moderate specificity proteins are those that were detected to varying degrees in both hemin–agarose and sepharose controls. Note that moderate specificity ranges from $\log_2$ ~1 (2-fold) to ~6 (~70-fold) enrichment on hemin–agarose versus sepharose. Color corresponds with the observed fold change in abundance between SA+ versus SA− conditions (from Fig. 2 data). Differential expression of proteins highly enriched non-specifically on spharose over hemin agarose ($\log_2$ ratios well below 0) are shown in dark blue (up reguated) and dark red (down regulated). Significance determined from three independent biological replicates. (C) Coomassie-stained SDS-PAGE showing gross enrichment of proteins on hemin–agarose versus sepharose controls. (D) Venn diagram showing the overlap between proteins enriched on hemin agarose over sepharose (Log_2 >1) in SA− versus SA+ conditions regardless of significance. (E) List of proteins with high hemin-agarose specificity found exclusively under SA− (red), SA+ (green), or both conditions (black). Note that the comparison was made between the high specificity class of one condition to all classes of the other condition. These therefore represent proteins uniquely detected in either condition. Boxed proteins were validated by immunoblotting (see 'validation of MS-identified HBPs visible only after heme depletion'). (See also Table S4.)

a wide variety of locations, including extracellular space, cytosol, mitochondrion, endoplasmic reticulum, and nucleus, suggesting that protein enrichment was not biased toward one cellular space versus another (Fig. S3). Strikingly, nearly half of the 213 proteins (~48%) were classified as RNA-binding proteins (Fig. S4). Gene ontology and KEGG pathway enrichment analysis further revealed a broad list of highly overlapping terms with false discovery rates well below the significance threshold ($Q < 0.05$) and with >5-fold enrichment (Fig. 5 and Table S5). We found that a vast majority of ontologies could be explained by physical interactions in protein complexes. For example, biological processes such as *SRP-dependent co-translational protein targeting to membrane*, *nuclear-transcribed mRNA catabolic process*, *viral gene expression*, and *translation initiation* (Fig. 5A); as well as cell components, such as the *polysome*, are linked to the ribosome core complex (Fig. 5B). Similarly, the highly enriched molecular function *threonine-type endopeptidase activity* (GO:004298) is linked to the 26s proteasome (Fig. 5C). In light of these and other observations, we evaluated

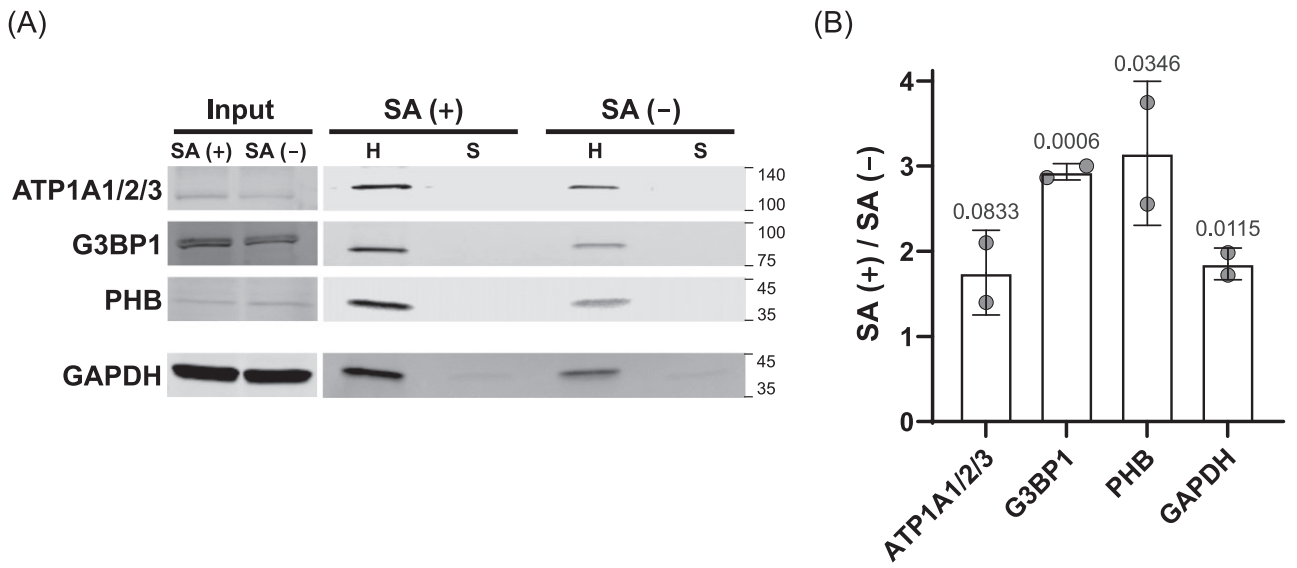

Fig. 4 Immunoblot validation of select proteins identified by DAsHA MS. A selected set of proteins identified as being hemin–agarose specific exclusively in the SA+ condition (ATP1A1/2/3; G3BP1; PHB) were validated by immunoblotting with protein-specific antibodies to confirm their hemin–agarose specificity. GAPDH, which is an established HBP, was evaluated in parallel as a control. (A) Representative immunoblot results for input and elution fractions after enrichment with hemin–agarose (H) versus sepharose (S). Note that the tendency for GAPDH to bind sepharose, visible as a band in the sepharose lanes, is also observed in the MS data (see Table S4). (B) Quantitative analysis comparing immunoblot signals from hemin–agarose bound proteins (H) in SA+ versus SA– conditions. The statistical significance for SA-dependent fold-enrichment on hemin–agarose was assessed using a one-tailed, two-sample t-test for each protein, and the calculated *P* values are indicated in the bar plot.

the mean node connectivity of each term, focusing on high-confidence protein interactions, which revealed a higher than average expected physical connectivity (i.e. *Node Degree in STRING*) for each term type and an overabundance of edges in the physical network across all 213 proteins (805 observed versus 352 expected edges; PPI enrichment *P*-value <1E-16) (Fig. 5D and Table S5).

We also observed significant enrichment of multiple KEGG pathways that harbor proteins detected by DAsHA. Most prominent of these was *systemic lupus erythematosus (KEGG ID: hsa05322)*, an ontological pathway linked to the presently untreatable autoimmune disease of the same name that includes nucleosomal histone proteins as well as specific spliceosome components that were detected by DAsHA (Fig. 5E). Notably, both spliceosome proteins, Snrpd1 and Snrpd3, undergo a significant increase in cellular abundance upon heme depletion with SA; and furthermore, Snrpd1 was detected with greater hemin–agarose specificity and greater significance in the SA+ condition, providing strong evidence for a role of heme in splicing and in diseases linked to splicing. We also observed significant enrichment in proteins associated with protein misfolding, including Parkinson's disease (KEGG ID: H00057), Prion disease (KEGG ID: H00061), and Amyotrophic lateral sclerosis (KEGG ID: H00058), within which we routinely observed mitochondrial ATP synthases Atp5f1b and Atp5f1c, among other proteins in the high hemin specificity class (Table S5). Similarly, we observed strong enrichment of multisystem proteinopathies (DOID:070355) in the *DISEASES* database, including heterogeneous nuclear ribonucleoproteins HNRNPA1 and HNRNPA2B1 and the transitional ATPase VCP (Fig. 5F).

Several functional protein complexes were revealed by DAsHA

Considering the high degree of protein–protein interaction in our dataset, we next explored whether functional protein complexes may be enriched by DAsHA. We found that 130 of the 213 STRING-mapped proteins (61%) participate in high-confidence physical protein interactions (Fig. 6A). Several distinctive clusters were enriched significantly within this dataset, which we further encapsulated with other proteins of similar function (Fig. 6B and Table S6; corresponding to color-coded clouds in panel A). Ribosomal and proteasomal complexes that have been established as heme interacting previously were the most prominently enriched functional complexes (Fig. 6B). Also prominent were nucleosomal histones H2B and H4 as well as nucleosome remodeling proteins and the spliceosome. Notably, H2B as well as multiple large ribosomal subunits and spliceosome proteins each exhibit a drastic increase in abundance upon heme depletion (Log_2 SA+/SA– > 5), suggesting a possible relationship between heme binding and abundance regulation for these proteins (Fig. S5). Significant enrichment was also noted for additional protein clusters involved in chaperone-mediated autophagy and protein folding, cytoskeleton and vesicular trafficking, and amino acid metabolism (Fig. 6A).

In most cases, we observed that HBPs identified via heme depletion alone (SA+) were found in clusters that were also identified without SA treatment. For example, in clusters associated with actin-binding/vesicle trafficking, ribosome, spliceosome, and DNA damage repair, we detected both proteins that require SA for hemin–agarose binding and others that could be detected regardless of SA treatment (Fig. 6C). In other cases, ontology terms were enriched only after SA treatment, such as the topoisomerases Top2a and Top2b involved in DNA replication and viral integration, as well as the sodium/potassium proton pumps Atp1a1 and Atp1a3. These data further convey the expansion of enriched gene ontologies afforded by DAsHA.

Many proteins enriched by hemin–agarose (39%) are not classified as having high confidence physical interactions in the STRING database, and in fact, we found a slight enrichment (1.3-fold) of SA+ specific proteins in this category (compare 41 to 31% in the set of 213 proteins).

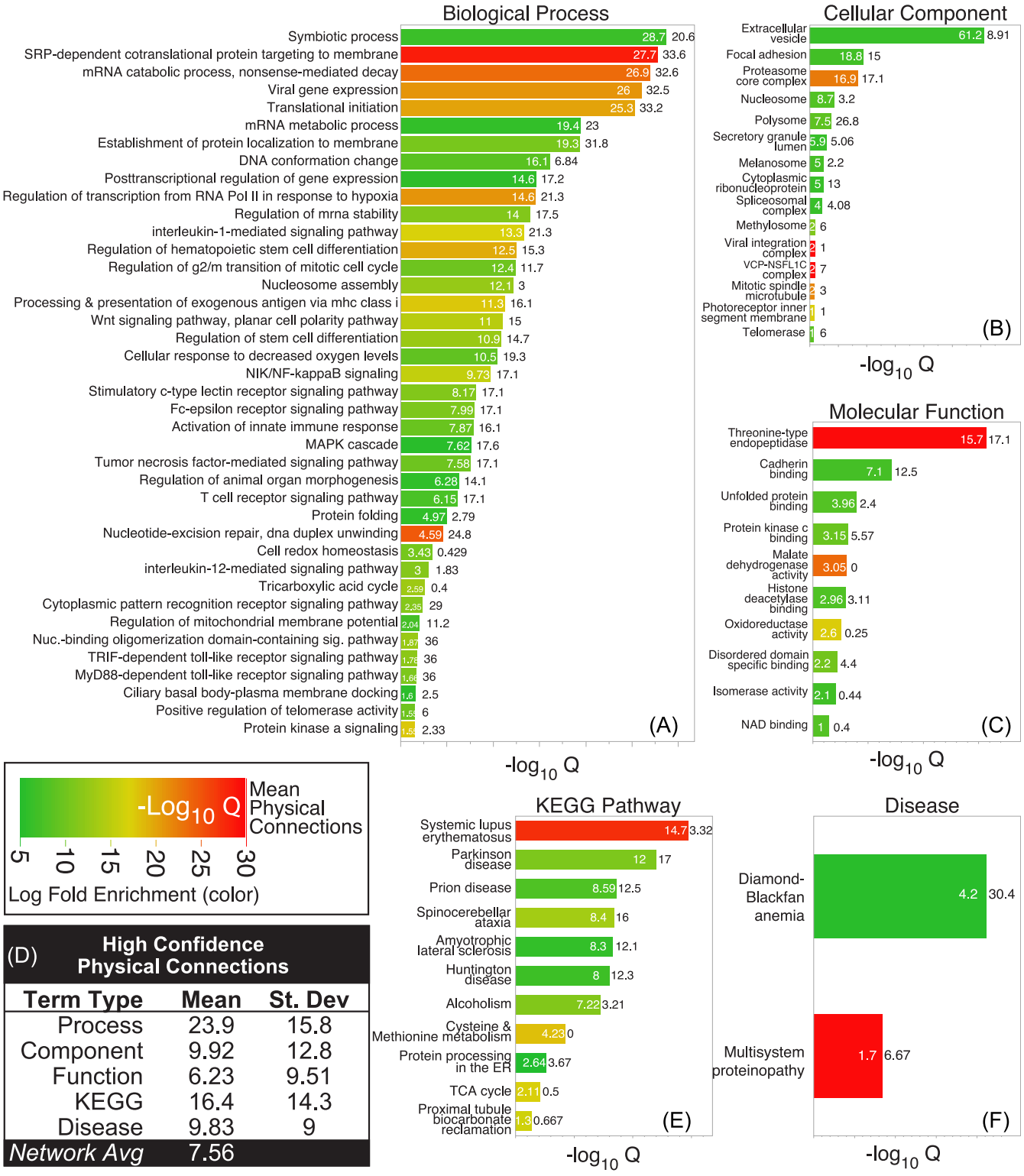

(D) **High Confidence Physical Connections**

Term Type	Mean	St. Dev
Process	23.9	15.8
Component	9.92	12.8
Function	6.23	9.51
KEGG	16.4	14.3
Disease	9.83	9
Network Avg	7.56	

Fig. 5 Ontological term enrichment of hemin-specific binding proteins. Gene ontology term enrichment for all moderate and high specificity proteins in SA– and SA+ conditions that were enriched above the significance threshold (–Log_{10} P-value >1.3): (A) biological process; (B) cellular component; (C) molecular function; (E) KEGG pathway; and (F) disease. Each graph shows a bar with embedded values (white numbers corresponding to the X-axis value) corresponding to the false discovery rate for the given ontological term. Black values outside each bar correspond to the mean physical connections observed for proteins within each term (corresponding to node degree in STRING). Bar color indicates log-fold enrichment (referred to as enrichment 'strength' in STRING). (D) Table of high confidence physical connections (min interaction score from STRING = 0.7) observed within each term type shown in A, B, C, E, and F. The average node degree for the entire network of high hemin–agarose specificity proteins (SA or SA+; 213 proteins) is shown for comparison. (See also Table S5.)

(A)

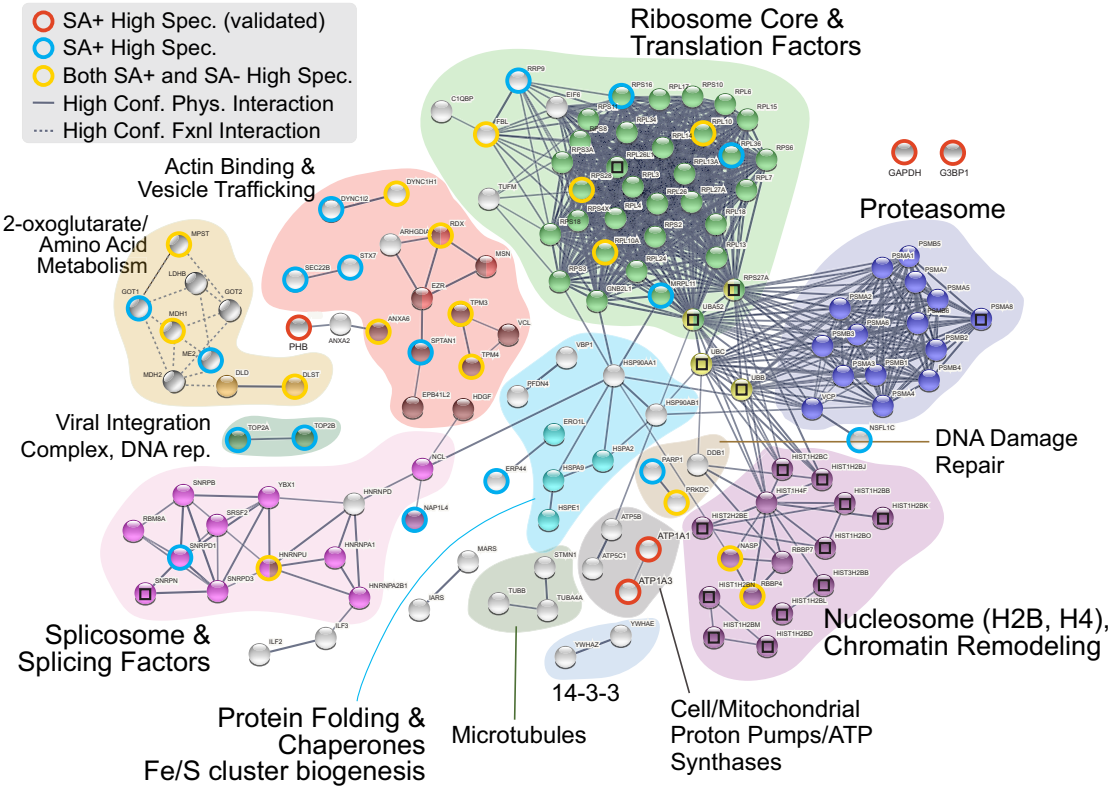

(B)

Ontological Category	GO-term	Description	Count in Network	Strength	False Discovery Rate	Color
Biological Process	GO.0006334	Nucleosome assembly	19 of 135	1.11	7.08E-13	
Biological Process	GO.0006103	2-oxoglutarate metabolic process	4 of 16	1.36	0.0024	
Biological Process	GO.2000643	Positve regulaton of early to late endosome transition	3 of 8	1.54	0.0074	
Biological Process	GO.0061077	Chaperone-mediated protein folding	5 of 55	0.92	0.0165	
Molecular Function	GO.0003779	Actin binding	14 of 438	0.47	0.0301	
Cellular Component	GO.0044391	Ribosomal subunit	33 of 178	1.23	7.75E-17	
Cellular Component	GO.0000502	Proteasome complex	15 of 62	1.35	1.87E-13	
Cellular Component	GO.0005681	Spliceosomal complex	12 of 192	0.76	6.67E-05	
Cellular Component	GO.0019035	Viral integration complex	2 of 2	1.96	0.0151	
Reactome Pathways	HAS-9613829	Chaperone-mediated autophagy	6 of 22	1.4	3.95E-06	

(C)

Physical Interaction Cluster	SA+ High Specificity	Both SA- & SA+ High Specificity	Total	# Members
Actin Binding & Vesicle Trafficking	4	5	9	15
Ribosome Core & Translation Factors	4	4	8	42
2-oxoglutarate/Amino Acid Metabolism*	2	3	5	9
Viral Integration Complex	2		2	2
Cell/Mitochondrial Proton Pumps	2		2	4
DNA Damage Repair	1	1	2	3
Spliceosome & Splicing Factors	1	1	2	11
Nucleosome & Assembly Factors		2	2	16
Proteasome				15
14-3-3				2
Microtubules				3
Protein Folding & Chaperones				8

Contains non-physical interactions

Fig. 6 Functional protein complexes identified by DAsHA MS. (A) Network of high confidence physical interactions between moderate or high hemin–agarose-specific proteins observed in SA– or SA+ conditions (213 proteins; min interaction score from STRING = 0.7). (See also Table S5.) Proteins were clustered using the MCL inflation method in STRING, and color-coded clouds were manually drawn to encapsulate notable clusters that also include functionally similar proteins not automatically grouped by ontology clustering. Spheres with embedded squares indicate proteins whose detectable peptides were shared with other protein identities (e.g. isoforms). Spheres encircled with red, blue, or yellow rings were detected in the high specificity class (exclusively detected from hemin–agarose but not sepharose enrichment), while spheres without rings were detected in the moderate specificity class (2–70-fold hemin–agarose versus sepharose enrichment). Not shown are most proteins unconnected by a high-confidence physical interaction unless they were explicitly validated (e.g. GAPDH and G3BP1). (B) Snapshot of the STRING network statistics also showing prominent ontologies that were explicitly enriched in the dataset of 213 proteins. Colors correspond to sphere colors in panel A. (C) Table showing the sum of high specificity proteins identified within each ontological cloud.

Most of these proteins could be broadly linked to general ontologies, including focal adhesion, mitochondrion/mitochondrial matrix, extracellular exosome, and metabolism where within high confidence functional interactions were noted for two oxoglutarate and amino acid metabolism ontologies that exhibited the greatest number of high confidence functional interactions (Fig. S6).

Discussion

We have conducted a comprehensive analysis of the heme interactome in human embryonic kidney cells and have expanded the ontological landscape that we understand as the *hemoproteome*. We employed a unique strategy, DAsHA, to improve enrichment of fractionally saturated HBPs that are otherwise difficult to enrich through traditional hemin–agarose chromatography. Coupled with SILAC quantitative MS, we significantly improved the capture and detection of hemin–agarose-specific binding proteins. The method, by design, did not capture known high affinity heme proteins and enzymes since our heme depletion strategy had more severe consequences on LH compared to total heme (Fig. 2A and B and Table S2). Rather, the method reveals what we consider to be proteins that interact with dynamic LH.

Through DaSHA, we have revealed a wide range of new proteins and functional protein complexes that associate with heme. While this study can distinguish specific versus non-specific heme-protein interactions, it cannot discern the functional mechanisms underlying these heme-protein interactions. Indeed, several questions emerge as to when heme-protein interactions that we have identified function as heme sinks that buffer toxic heme levels, as heme trafficking agents that facilitate the controlled movement of heme through the cell, or as targets of heme-dependent protein regulation. Our study provides a relatively broad list of protein types and functional complexes that are consistent with emerging evidence of heme's roles in genome, transcriptome, and proteome regulation. Ongoing efforts to tease apart the various roles of the heme-protein interactome will nonetheless be necessary to discern the importance of these interactions to the cell.

Heme, chromatin remodeling, and DNA repair

This study has revealed several previously unknown interactions between heme and nucleosomal histones H2B and H4, as well as nucleosome remodeling proteins (Fig. 6). We have further shown that variants of histone H2B, which bind with specificity to hemin–agarose, also undergo a dramatic increase in expression upon heme depletion (Figs 2 and 3). Taken together, these observations suggest that histone proteins are not only sensitive to cellular heme levels but also capable of physically associating with the porphyrin molecule. The direct effects of heme are yet to be determined; however, there is prior evidence for both indirect and direct roles of heme in chromatin remodeling. Indirect evidence has shown that DNA accessibility at promoter regions (measured by a transposon accessibility sequencing assay) is altered under low heme conditions resulting in changes in gene transcription.[54] In contrast, direct heme binding to Gis1, a yeast transcription factor and histone demethylase orthologous to the mammalian JMJD2/KDM4 family of demethylases, has been shown to regulate genes involved in the oxidative stress response and carbon metabolism via post-diauxic shift elements in the promoters of numerous genes activities.[13] Whether the functional utility of the heme-histone interaction observed in our study serves a direct regulatory versus an indirect LH-buffering role remains unknown, warranting further investigation.

We have also identified connections between heme and DNA repair proteins that could suggest a role for heme binding in the control of genome integrity. Specifically, we observed specific heme binding to proteins associated with nucleotide excision and base excision repair processes, including Ddb1 and Parp1, as well as a protein kinase sensor of DNA damage, Prkdc (Fig. 6). We also found HBPs associated with DNA replication, such as helicases (e.g. G3BP1), topoisomerases (e.g. Top2a and Top2b), and mitochondrial single-stranded binding protein (Ssbp1). Taken together, these data suggest that heme may have a direct role in genome integrity that relies on specific heme-protein interactions involved in the detection and repair of DNA damage. Consistent with these observations, previous reports have shown that dysregulated heme is involved in both DNA damaging and protective responses. Excess LH is known to induce DNA damage,[24–26,55] but has also been shown to bind DNA-protective proteins from starved cells (known as *DPs*) to protect DNA from damage in bacteria.[56] Similarly, mice lacking the heme-degrading enzyme HO-1, undergo dysregulated expression of histone γ-H2A and increased DNA damage due to altered ATM-dependent DNA repair.[57] In many of these cases, a direct role for heme has not been identified, and therefore studies such as ours may provide potential hypotheses for dissecting direct versus indirect roles of heme.

Heme and RNA splicing

We observed several RNA processing proteins that bind specifically to hemin–agarose. For example, we discovered proteins involved in tRNA and rRNA processing, such as ThumpD1 and FBL, and in RNA stability, such as SSB (Table S4). However, most notable were proteins involved in mRNA splicing and packaging, including multiple snRNPs and hnRNPs (Fig. 6). Ours is not the first to find an association between heme in RNA processing. For example, transcriptome-wide analyses of patients with myelodysplasia, wherein aberrant splicing is common, recently revealed that heme biosynthesis is a major target of aberrant splicing caused by mutations in spliceosome subunit Sf3b1.[58] A report published in tandem showed that the long non-coding RNA, UCA1, effectively stabilizes the mRNA of Alas1 (a key heme biosynthetic enzyme) through a direct interaction with splicing factor Hnrnp1, thereby promoting heme biosynthesis.[59] Mounting evidence has also shown that heme regulates microRNA processing proteins such as DGCR8.[60–65] Our results provide evidence that spliceosomal factors interact with heme, and therefore further work to determine if this interaction plays a regulatory role or not in splicing is necessary. Taken together, ours and previously published evidence provide growing evidence that heme may influence core RNA processing functions.

Heme and proteostasis

Heme's control of protein abundance is achieved through a variety of mechanisms. In some cases, heme–protein interactions are essential for maintaining the stability of the HBP. For example, the interaction between hemoglobin and heme is essential not only for oxygen transport but also to maintain stability of the protein itself.[48] In other cases, heme promotes protein degradation, as in the case of Alas1, wherein heme functions as a feedback signal triggering ubiquitin-mediated degradation of the protein.[49] We identified Got1 and Got2 aspartate aminotransferases as highly specific hemin–agarose binding proteins that were also unique to the SA+ heme depleted condition (Fig. 6). These proteins

are essential for the interconversion of glutamate from aspartate or cysteine, each of which is a destabilizing residue in the N-end rule pathway. Previous work has shown that heme functions as a stoichiometric and catalytic down-regulator of the N-end rule pathway by altering arginylation rates for oxidized cysteine, aspartate, and glutamate N-terminal residues that drive degradation by N-end rule E3 ubiquitin ligases.[66] Similarly, heme interacts directly with the 26S proteasome and controls its activity under hyper-elevated heme stress.[67]

Heme, the ribosome, and other RNA-binding proteins

Heme has recently been shown to bind the ribosome both *in vitro* and *in vivo* by association with rRNA G-quadruplexes (G4s).[38] G4s form in the ribosomal RNAs of birds and mammals. The interactions of these G4s with heme are currently thought to serve as a buffer for LH that may in turn regulate heme metabolism and trafficking. This study combined with our previous work and published evidence from other labs has confirmed this interaction through the enrichment of large and small ribosomal subunits (Fig. 6).[40] We suspect that ribosome/heme interactions are captured in part through heme/G4 as opposed to heme-protein interactions, although several ribosomal subunits harbor putative heme regulatory motifs (HRMs) that suggest ribosomal protein-heme interactions are also possible.[40] Indeed, a hemin-affinity-based approach such as the one used here cannot distinguish between protein versus non-protein-based interactions, nor can it distinguish between direct and indirect interactions, and therefore the enrichment of functional protein complexes could be facilitated by both heme-direct and indirect interactions. Whether the prominent interactions between heme and the ribosome alter the functionality of or confer a distinctive function for the ribosome remains unknown. However, we have also identified several putative HBPs that serve accessory roles in protein translation, such as aminoacyl tRNA synthetases such as IARS and MARS that are essential for the formation of charged isoleucyl and methionyl tRNA, among other tRNA and rRNA processing enzymes described above. Whether these interactions are simply to buffer excess LH or serve more regulatory functions are of great interest and ongoing work.

Emerging evidence for heme-RNA-protein interactions such as those within the ribosome suggests that the RNA-binding subset of the proteome may be a particular target for heme-based regulation. For example, long non-coding RNAs also adopt G4 structures,[68] interact with proteins, and can regulate heme biosynthesis,[59] which suggests a possible role for heme in these RNA/protein interactions. In support of this hypothesis, we found that 48% of all proteins identified in the collection of hemin–agarose-specific SA+/− results (102/213 proteins) are classified as RNA binding (GO:0003723; 5.6x enrichment; $Q < 3.24E\text{-}47$) (Fig. S4). Most of these RNA-binding proteins (69/102) are not ribosomal proteins, suggesting the possibility that heme may interface with several of the identified targets through an RNA intermediary in addition to or in place of direct heme-protein interaction.

Involvement of heme in post-translational processes

We discovered hemin–agarose-specific interactions with proteins involved in a wide range of post-translational processes, including protein-vesicle trafficking, chaperone mediated protein folding, and energy metabolism. Heme has been proposed to be biodistributed as cargo in vesicular trafficking pathways between the mitochondrion, ER, Golgi, and plasma membrane.[9,37,69–71] We found prominent and specific enrichment of cytoskeletal proteins involved in endosomal trafficking to the plasma membrane, trafficking from the plasma membrane to early endosomes, as well as proteins involved in cell polarity, movement, and mitosis (Fig. 6 and Table S6).

We observed several cytoplasmic and mitochondrial heat shock proteins in our analysis (Fig. 6 and Table S6). In addition to their well-established roles in protein folding, quality control, and stress response,[72] HSPs are also involved in iron-sulfur cluster biogenesis, important for heme biosynthesis,[73] and in facilitating catalytic activities, including intra-protein electron transfer to heme cofactors.[74] Of note, HSPs have also been directly implicated in heme insertion into hemoproteins. For example, Hsp90 interacts with and is required for heme insertion into hemoglobin,[75] nitric oxide synthase,[76] and soluble guanylate cyclase.[77] Heme has an established role in stabilizing protein folding of HBPs.[78] Additionally, through its cytotoxic ability to promote the formation of reactive oxygen species and to promote Nrf2-mediated transcription of redox stress response genes, excess LH can promote protein misfolding and aggregation.[79]

Conclusions

DAsHA is a new approach that seeks to discover novel hemoproteins by depleting endogenous HBPs of their heme to enhance their enrichment through traditional hemin–agarose chromatography. By abolishing exchange LH, but not total heme, we sought to identify proteins that constitute the network of labile HBPs. Indeed, our approach did not identify canonical high affinity heme proteins, but rather uncovered an array of previously unknown HBPs, thereby expanding the known landscape of the hemoproteome. While we identified GAPDH in our studies, a protein previously implicated in heme trafficking, we did not identify known heme transporters, HRG1,[80] FLVCR1,[81] and FLVCR2,[82] or heme trafficking factors like PGRMC1 and PGRMC2.[83] FLVCR2 and HRG1 were not identified since peptides from these proteins were not detected at the WP-level. On the other hand, peptides from PGRMC1/2 and FLVCR1 were detected at the WP-level, but not found associated with hemin–agarose, possibly because the heme propionates, which are used in the conjugation of heme to the hemin–agarose resin, are unavailable for interactions with proteins that require such engagement,[84,85] as is the case for PGRMC1/2.[86]

Our approach is biased toward identifying HBPs that conditionally bind hemin–agarose when cells are depleted of LH using SA and that are competitively eluted with imidazole. Both forms of selection favor proteins that have exchangeable heme binding sites. Indeed, if imidazole cannot elute a protein from hemin–agarose, it is, by definition, a non-exchangeable heme binding site, at least with respect to imidazole competition. Our approach may not identify very low affinity hemoproteins or ones that only transiently interact with heme. Other complementary hemoproteomics approaches may be better suited to identify transient heme interacting proteins, such as employing the use of diazirine conjugated heme analogs that can be covalently crosslinked to proteins upon exposure to UV light.[87]

Our approach is also not suited to identify proteins that interact with heme primarily through porphyrin-protein hydrophobic interactions as they may not be eluted from hemin–agarose resin with imidazole. However, given that heme-iron axial coordination is a dominant contributor to heme–protein interactions,[88] and a hallmark of *bona fide* hemoproteins as

evidenced by the overwhelming majority of structurally and spectroscopically characterized heme enzymes, trafficking factors, and targets of heme signaling,[3,89,90] it is unlikely that proteins that interact with hemin–agarose primarily via hydrophobic interactions will be physiologically relevant. Nevertheless, our workflow can be easily adapted to include comparisons between proteins that elute from hemin–agarose using heat or chemical denaturation versus imidazole to potentially reveal proteins that interact with heme primarily via hydrophobic interactions. Alternatively, a comparison between proteins eluted from hemin–agarose versus protoporphyrin–agarose resins may also reveal hemoproteins in which hydrophobic interactions dominate.

It remains to be determined if a subset of the HBPs identified in this study play roles in heme homeostasis or novel heme-dependent or regulated factors. The identification of putative signatures of HRMs,[3,91–95] and the development of computational tools to predict such heme binding sites,[96] can help guide future work to establish functional consequences of heme binding to the HBPs identified here. Additionally, given that different cell types have different metabolic demands for heme, future work is required to establish how the putative hemoproteins identified in this study across diverse ontological classes are coordinated to support heme regulated signaling and physiology.

Our studies are complemented by Tsolaki *et al.*, in which heme interacting proteins were identified from cells in the presence versus absence of excess hemin (as opposed to our work in which heme is depleted below physiological conditions).[40] Overlap between the two datasets provides a view of similarities and differences that not only underscore reproducibility of shared findings but also highlight unique findings that were achieved only through heme depletion. Shared findings between the two studies include heat shock proteins, cytoskeletal proteins, ATP synthases, heterogeneous ribonucleoproteins, proteasomal subunits, splicing factors, and the DNA damage response protein Ddb1. Several unique findings from our work, therefore, include proteins involved in vesicular trafficking, nucleosome and nucleosome remodeling, the spliceosome, and DNA replication (Fig. 6). In many of these cases, we observed enrichment only upon heme depletion, supporting the conclusion that DAsHA can provide a unique view into the heme-binding subset of the human proteome and can complement other proteomics approaches.

Supplementary material

Supplementary data are available at *Metallomics* online.

Funding

We acknowledge support from US National Institutes of Health (NIH) grants GM118744 (to A.R.R. and M.P.T.), GM117400 (to M.P.T.), GM145350 (to A.R.R.), ES025661 (to A.R.R.), NS123168 (to A.R.R.), a US National Science Foundation (NSF) grant 1552791 (to A.R.R.), and the Georgia Institute of Technology Blanchard and Vasser-Woolley fellowships (to A.R.R.).

Conflicts of interest

There are no conflicts of interest to declare.

Data availability

All data from this study are included in the manuscript and/or supporting information, and all mass spectrometry proteomics data have been deposited into the ProteomeXchange Consortium [http://www.proteomexchange.org] via the PRIDE partner repository [https://www.ebi.ac.uk/pride/] with the dataset identifier PXD037165.

References

1. S. Hou, M. F. Reynolds, F. T. Horrigan, S. H. Heinemann and T. Hoshi, Reversible binding of heme to proteins in cellular signal transduction, *Acc. Chem. Res.* 2006, 39(12), 918–924.
2. T. Kühl and D. Imhof, Regulatory Fe(II/III) heme: the reconstruction of a molecule's biography, *ChemBioChem* 2014, 15(14), 2024–2035.
3. A. Wißbrock, A. A. Paul George, H. H. Brewitz, T. Kühl and D. Imhof, The molecular basis of transient heme-protein interactions: analysis, concept and implementation, *Biosci. Rep.* 2019, 39(1), BSR20181940.
4. S. M. Mense and L. Zhang, Heme: a versatile signaling molecule controlling the activities of diverse regulators ranging from transcription factors to MAP kinases, *Cell Res.*, 2006, 16(8), 681–692.
5. T. L. Poulos, Heme enzyme structure and function, *Chem. Rev.*, 2014, 114(7), 3919–3962.
6. I. G. Chambers, M. M. Willoughby, I. Hamza and A. R. Reddi, One ring to bring them all and in the darkness bind them: the trafficking of heme without deliverers, *Biochim. Biophys. Acta –Mol. Cell Res.*, 2021, 1868(1), 118881.
7. R. K. Donegan, C. M. Moore, D. A. Hanna and A. R. Reddi, Handling heme: the mechanisms underlying the movement of heme within and between cells, *Free Radical Biol. Med.*, 2019, 133, 88–100.
8. D. A. Hanna, O. Martinez-Guzman and A. R. Reddi, Heme gazing: illuminating eukaryotic heme trafficking, dynamics, and signaling with fluorescent heme sensors, *Biochemistry*, 2017, 56(13), 1815–1823.
9. A. R. Reddi and I. Hamza, Heme mobilization in animals: a metallolipid's journey, *Acc. Chem. Res.*, 2016, 49(6), 1104–1110.
10. K. Ogawa, Heme mediates derepression of Maf recognition element through direct binding to transcription repressor Bach1, *EMBO J.*, 2001, 20(11), 2835–2843.
11. M. J. Hickman and F. Winston, Heme levels switch the function of Hap1 of *Saccharomyces cerevisiae* between transcriptional activator and transcriptional repressor, *Mol. Cell. Biol.*, 2007, 27(21), 7414–7424.
12. L. Yin, N. Wu, J. C. Curtin, M. Qatanani, N. R. Szwergold, R. A. Reid, G. M. Waitt, D. J. Parks, K. H. Pearce, G. B. Wisely and M. A. Lazar, Rev-erbalpha, a heme sensor that coordinates metabolic and circadian pathways, *Science* 2007, 318(5857), 1786–1789.
13. Y. Zenke-Kawasaki, Y. Dohi, Y. Katoh, T. Ikura, M. Ikura, T. Asahara, F. Tokunaga, K. Iwai and K. Igarashi, Heme induces ubiquitination and degradation of the transcription factor Bach1, *Mol. Cell. Biol.*, 2007, 27(19), 6962–6971.
14. L. Zhang and A. Hach, Molecular mechanism of heme signaling in yeast: the transcriptional activator Hap1 serves as the key mediator, *Cell. Mol. Life Sci.*, 1999, 56(5-6), 415–426.
15. K. Pfeifer, K. S. Kim, S. Kogan and L. Guarente, Functional dissection and sequence of yeast HAP1 activator, *Cell*, 1989, 56(2), 291–301.
16. Y. Zhu, T. Hon, W. Ye and L. Zhang, Heme deficiency interferes with the Ras-mitogen-activated protein kinase signaling pathway and expression of a subset of neuronal genes, *Cell Growth Differ. Mol. Biol. J. Am. Assoc. Cancer Res.*, 2002, 13(9), 431–439.
17. B. Alvarez-Castelao, S. tom Dieck, C. M. Fusco, P. Donlin-Asp, J. D. Perez and E. M. Schuman, The switch-like expression of heme-regulated kinase 1 mediates neuronal proteostasis following proteasome inhibition, *eLife*, 2020, 9, e52714.

18. B. F. Schmalohr, A. - H. M. Mustafa, O. H. Krämer and D. Imhof, Structural insights into the interaction of heme with protein tyrosine kinase JAK2*, *ChemBioChem*, 2021, 22(5), 861–864.
19. A. P. Han, C. Yu, L. Lu, Y. Fujiwara, C. Browne, G. Chin, M. Fleming, P. Leboulch, S. H. Orkin and J. J. Chen, Heme-regulated eIF2alpha kinase (HRI) is required for translational regulation and survival of erythroid precursors in iron deficiency, *EMBO J.*, 2001, 20(23), 6909–6918.
20. J. D. Belcher, C. Chen, J. Nguyen, L. Milbauer, F. Abdulla, A. I. Alayash, A. Smith, K. A. Nath, R. P. Hebbel and G. M. Vercellotti, Heme triggers TLR4 signaling leading to endothelial cell activation and vaso-occlusion in murine sickle cell disease, *Blood*, 2014, 123(3), 377–390.
21. F. T. Horrigan, S. H. Heinemann and T. Hoshi, Heme regulates allosteric activation of the Slo1 BK channel, *J. Gen. Physiol.*, 2005, 126(1), 7–21.
22. M. J. Burton, S. M. Kapetanaki, T. Chernova, A. G. Jamieson, P. Dorlet, J. Santolini, P. C. E. Moody, J. S. Mitcheson, N. W. Davies, R. Schmid, E. L. Raven and N. M. Storey, A heme-binding domain controls regulation of ATP-dependent potassium channels, *Proc. Natl. Acad. Sci.*, 2016, 113(14), 3785–3790.
23. M. J. Burton, J. Cresser-Brown, M. Thomas, N. Portolano, J. Basran, S. L. Freeman, H. Kwon, A. R. Bottrill, M. J. Llansola-Portoles, A. A. Pascal, R. Jukes-Jones, T. Chernova, R. Schmid, N. W. Davies, N. M. Storey, P. Dorlet, P. C. E. Moody, J. S. Mitcheson and E. L. Raven, Discovery of a heme-binding domain in a neuronal voltage-gated potassium channel, *J. Biol. Chem.*, 2020, 295(38), 13277–13286.
24. D. Chiabrando, F. Vinchi, V. Fiorito, S. Mercurio and E. Tolosano, Heme in pathophysiology: a matter of scavenging, metabolism and trafficking across cell membranes, *Front. Pharmacol.*, 2014, 5, 61.
25. S. Sassa, Why heme needs to be degraded to iron, biliverdin IX-alpha, and carbon monoxide?, *Antioxid. Redox. Signal.*, 2004, 6(5), 819–824.
26. S. Kumar and U. Bandyopadhyay, Free heme toxicity and its detoxification systems in human, *Toxicol. Lett.*, 2005, 157(3), 175–188.
27. G. C. - H. Leung, S. S. - P. Fung, A. E. Gallio, R. Blore, D. Alibhai, E. L. Raven and A. J. Hudson, Unravelling the mechanisms controlling heme supply and demand, *Proc. Natl. Acad. Sci.*, 2021, 118(22), e2104008118.
28. A. E. Gallio, S. S. - P. Fung, A. Cammack-Najera, A. J. Hudson and E. L. Raven, Understanding the logistics for the distribution of heme in cells, *JACS Au*, 2021, 1(10), 1541–1555.
29. D. A. Hanna, R. M. Harvey, O. Martinez-Guzman, X. Yuan, B. Chandrasekharan, G. Raju, F. W. Outten, I. Hamza and A. R. Reddi, Heme dynamics and trafficking factors revealed by genetically encoded fluorescent heme sensors, *Proc. Natl. Acad. Sci.*, 2016, 113(27), 7539–7544.
30. M. - T. Hopp, B. F. Schmalohr, T. Kühl, M. S. Detzel, A. Wißbrock and D. Imhof, Heme determination and quantification methods and their suitability for practical applications and everyday use, *Anal. Chem.*, 2020, 92(14), 9429–9440.
31. J. R. Abshire, C. J. Rowlands, S. M. Ganesan, P. T. C. So and J. C. Niles, Quantification of labile heme in live malaria parasites using a genetically encoded biosensor, *Proc. Natl. Acad. Sci. U S A*, 2017, 114(11), E2068—E2076.
32. S. Xu, H. - W. Liu, L. Chen, J. Yuan, Y. Liu, L. Teng, S. - Y. Huan, L. Yuan, X. - B. Zhang and W. Tan, Learning from artemisinin: bioinspired design of a reaction-based fluorescent probe for the selective sensing of labile heme in complex biosystems, *J. Am. Chem. Soc.*, 2020, 142(5), 2129–2133.
33. X. Yuan, N. Rietzschel, H. Kwon, A. B. Walter Nuno, D. A. Hanna, J. D. Phillips, E. L. Raven, A. R. Reddi and I. Hamza, Regulation of intracellular heme trafficking revealed by subcellular reporters, *Proc. Natl. Acad. Sci.*, 2016, 113(35), E5144–E5152.
34. Y. Song, M. Yang, S. V. Wegner, J. Zhao, R. Zhu, Y. Wu, C. He and P. R. Chen, A genetically encoded FRET sensor for intracellular heme, *ACS Chem. Biol.*, 2015, 10(7), 1610–1615.
35. K. Kawai, T. Hirayama, H. Imai, T. Murakami, M. Inden, I. Hozumi and H. Nagasawa, Molecular imaging of labile heme in living cells using a small molecule fluorescent probe, *J. Am. Chem. Soc.*, 2022, 144(9), 3793–3803.
36. E. A. Sweeny, A. B. Singh, R. Chakravarti, O. Martinez-Guzman, A. Saini, M. M. Haque, G. Garee, P. D. Dans, L. Hannibal, A. R. Reddi and D. J. Stuehr, Glyceraldehyde-3-phosphate dehydrogenase is a chaperone that allocates labile heme in cells, *J. Biol. Chem.*, 2018, 293(37), 14557–14568.
37. O. Martinez-Guzman, M. M. Willoughby, A. Saini, J. V. Dietz, I. Bohovych, A. E. Medlock, O. Khalimonchuk and A. R. Reddi, Mitochondrial-nuclear heme trafficking in budding yeast is regulated by GTPases that control mitochondrial dynamics and ER contact sites, *J. Cell Sci.*, 2020, 133(10), jcs237917.
38. S. Mestre-Fos, C. Ito, C. M. Moore, A. R. Reddi and L. D. Williams, Human ribosomal G-quadruplexes regulate heme bioavailability, *J. Biol. Chem.*, 2020, 295(44), 14855–14865.
39. D. A. Hanna, R. Hu, H. Kim, O. Martinez-Guzman, M. P. Torres and A. R. Reddi, Heme bioavailability and signaling in response to stress in yeast cells, *J. Biol. Chem.*, 2018, 293(32), 12378–12393.
40. V. C. Tsolaki, S. K. Georgiou-Siafis, A. I. Tsamadou, S. A. Tsiftsoglou, M. Samiotaki, G. Panayotou and A. S. Tsiftsoglou, Hemin accumulation and identification of a heme-binding protein clan in K562 cells by proteomic and computational analysis, *J. Cell. Physiol.*, 2022, 237(2), 1315–1340.
41. C. Andreini, V. Putignano, A. Rosato and L. Banci, The human iron-proteome†, *Metallomics*, 2018, 10(9), 1223–1231.
42. N. Wang, J. Zhang, L. Zhang, X. - Y. Yang, N. Li, G. Yu, J. Han, K. Cao, Z. Guo, X. Sun and X. - Y. He, Proteomic analysis of putative heme-binding proteins in Streptococcus pyogenes, *Metallomics*, 2014, 6(8), 1451.
43. D. A. Hanna, C. M. Moore, L. Liu, X. Yuan, I. M. Dominic, A. S. Fleischhacker, I. Hamza, S. W. Ragsdale and A. R. Reddi, Heme oxygenase-2 (HO-2) binds and buffers labile ferric heme in human embryonic kidney cells, *J. Biol. Chem.*, 2022, 298(2), 101549.
44. H. - C. Chien, A. A. Zur, T. S. Maurer, S. W. Yee, J. Tolsma, P. Jasper, D. O. Scott and K. M. Giacomini, Rapid method to determine intracellular drug concentrations in cellular uptake assays: application to metformin in organic cation transporter 1-transfected human embryonic kidney 293 cells, *Drug Metab. Dispos.*, 2016, 44(3), 356–364.
45. Z. Weissman, M. Pinsky, R. K. Donegan, A. R. Reddi and D. Kornitzer, Using genetically encoded heme sensors to probe the mechanisms of heme uptake and homeostasis in Candida albicans, *Cell. Microbiol.*, 2021, 23(2), e13282.
46. J. V. Dietz, M. M. Willoughby, R. B. Piel, T. A. Ross, I. Bohovych, H. G. Addis, J. L. Fox, W. N. Lanzilotta, H. A. Dailey, J. A. Wohlschlegel, A. R. Reddi, A. E. Medlock and O. Khalimonchuk, Mitochondrial contact site and cristae organizing system (MICOS) machinery supports heme biosynthesis by enabling optimal performance of ferrochelatase, *Redox. Biol.*, 2021, 46, 102125.
47. L. Liu, A. B. Dumbrepatil, A. S. Fleischhacker, E. N. G. Marsh and S. W. Ragsdale, Heme oxygenase-2 is post-translationally regulated by heme occupancy in the catalytic site, *J. Biol. Chem.*, 2020, 295(50), 17227–17240.

48. I. S. Pires, D. A. Belcher and A. F. Palmer, Quantification of active apohemoglobin heme-binding sites via dicyanohemin incorporation, *Biochemistry*, 2017, 56(40), 5245–5259.
49. Y. Kubota, K. Nomura, Y. Katoh, R. Yamashita, K. Kaneko and K. Furuyama, Novel mechanisms for heme-dependent degradation of ALAS1 protein as a component of negative feedback regulation of heme biosynthesis, *J. Biol. Chem.*, 2016, 291(39), 20516–20529.
50. R. Chakravarti, K. S. Aulak, P. L. Fox and D. J. Stuehr, GAPDH regulates cellular heme insertion into inducible nitric oxide synthase, *Proc. Natl. Acad. Sci.*, 2010, 107(42), 18004–18009.
51. L. Hannibal, D. Collins, J. Brassard, R. Chakravarti, R. Vempati, P. Dorlet, J. Santolini, J. H. Dawson and D. J. Stuehr, Heme binding properties of glyceraldehyde-3-phosphate dehydrogenase, *Biochemistry*, 2012, 51(43), 8514–8529.
52. P. Biswas, Y. Dai and D. J. Stuehr, Indoleamine dioxygenase and tryptophan dioxygenase activities are regulated through GAPDH- and Hsp90-dependent control of their heme levels, *Free Radical Biol. Med.*, 2022, 180, 179–190.
53. B. Tupta, E. Stuehr, M. P. Sumi, E. A. Sweeny, B. Smith, D. J. Stuehr and A. Ghosh, GAPDH is involved in the heme-maturation of myoglobin and hemoglobin, *FASEB J. Off. Publ. Fed. Am. Soc. Exp. Biol.*, 2022, 36(2), e22099.
54. R. Liao, Y. Zheng, X. Liu, Y. Zhang, G. Seim, N. Tanimura, G. M. Wilson, P. Hematti, J. J. Coon, J. Fan, J. Xu, S. Keles and E. H. Bresnick, Discovering how heme controls genome function through heme-omics, *Cell Rep.*, 2020, 31(13), 107832.
55. S. Ishikawa, S. Tamaki, M. Ohata, K. Arihara and M. Itoh, Heme induces DNA damage and hyperproliferation of colonic epithelial cells via hydrogen peroxide produced by heme oxygenase: a possible mechanism of heme-induced colon cancer, *Mol. Nutr. Food Res.*, 2010, 54(8), 1182–1191.
56. J. - L. Gao, Y. Lu, G. Browne, B. C. - M. Yap, J. Trewhella, N. Hunter and K. - A. Nguyen, The role of heme binding by DNA-protective protein from starved cells (Dps) in the tolerance of porphyromonas gingivalis to heme toxicity, *J. Biol. Chem.*, 2012, 287(50), 42243–42258.
57. L. E. Otterbein, A. Hedblom, C. Harris, E. Csizmadia, D. Gallo and B. Wegiel, Heme oxygenase-1 and carbon monoxide modulate DNA repair through ataxia-telangiectasia mutated (ATM) protein, *Proc. Natl. Acad. Sci.*, 2011, 108(35), 14491–14496.
58. Y. Shiozawa, L. Malcovati, A. Gallì, A. Sato-Otsubo, K. Kataoka, Y. Sato, Y. Watatani, H. Suzuki, T. Yoshizato, K. Yoshida, M. Sanada, H. Makishima, Y. Shiraishi, K. Chiba, E. Hellström-Lindberg, S. Miyano, S. Ogawa and M. Cazzola, Aberrant splicing and defective mRNA production induced by somatic spliceosome mutations in myelodysplasia, *Nat. Commun.*, 2018, 9(1), 3649.
59. J. Liu, Y. Li, J. Tong, J. Gao, Q. Guo, L. Zhang, B. Wang, H. Zhao, H. Wang, E. Jiang, R. Kurita, Y. Nakamura, O. Tanabe, J. D. Engel, E. H. Bresnick, J. Zhou and L. Shi, Long non-coding RNA-dependent mechanism to regulate heme biosynthesis and erythrocyte development, *Nat. Commun.*, 2018, 9(1), 4386.
60. S. H. Weitz, M. Gong, I. Barr, S. Weiss and F. Guo, Processing of microRNA primary transcripts requires heme in mammalian cells, *Proc. Natl. Acad. Sci.*, 2014, 111(5), 1861–1866.
61. J. Quick-Cleveland, J. P. Jacob, S. H. Weitz, G. Shoffner, R. Senturia and F. Guo, The DGCR8 RNA-binding heme domain recognizes primary microRNAs by clamping the hairpin, *Cell Rep.*, 2014, 7(6), 1994–2005.
62. I. Barr, A. T. Smith, Y. Chen, R. Senturia, J. N. Burstyn and F. Guo, Ferric, not ferrous, heme activates RNA-binding protein DGCR8 for primary microRNA processing, *Proc. Natl. Acad. Sci.*, 2012, 109(6), 1919–1924.
63. A. C. Partin, T. D. Ngo, E. Herrell, B. - C. Jeong, G. Hon and Y. Nam, Heme enables proper positioning of Drosha and DGCR8 on primary microRNAs, *Nat. Commun.*, 2017, 8(1), 1737.
64. H. M. Girvan, J. M. Bradley, M. R. Cheesman, J. R. Kincaid, Y. Liu, K. Czarnecki, K. Fisher, D. Leys, S. E. J. Rigby and A. W. Munro, Analysis of heme iron coordination in DGCR8: the heme-binding component of the microprocessor complex, *Biochemistry*, 2016, 55(36), 5073–5083.
65. M. Faller, M. Matsunaga, S. Yin, J. A. Loo and F. Guo, Heme is involved in microRNA processing, *Nat. Struct. Mol. Biol.*, 2007, 14(1), 23–29.
66. R. - G. Hu, H. Wang, Z. Xia and A. Varshavsky, The N-end rule pathway is a sensor of heme, *Proc. Natl. Acad. Sci.*, 2008, 105(1), 76–81.
67. F. Vallelian, J. W. Deuel, L. Opitz, C. A. Schaer, M. Puglia, M. Lönn, W. Engelsberger, S. Schauer, E. Karnaukhova, D. R. Spahn, R. Stocker, P. W. Buehler and D. J. Schaer, Proteasome inhibition and oxidative reactions disrupt cellular homeostasis during heme stress, *Cell Death Differ.*, 2015, 22(4), 597–611.
68. X. Mou, S. W. Liew and C. K. Kwok, Identification and targeting of G-quadruplex structures in *MALAT1* long non-coding RNA, *Nucleic Acids Res.*, 2022, 50(1), 397–410.
69. S. Severance and I. Hamza, Trafficking of heme and porphyrins in metazoa, *Chem. Rev.*, 2009, 109(10), 4596–4616.
70. A. Sobh, A. Loguinov, J. Zhou, S. Jenkitkasemwong, R. Zeidan, N. El Ahmadie, A. Tagmount, M. Knutson, P. G. Fraenkel and C. D. Vulpe, Genetic screens reveal CCDC115 as a modulator of erythroid iron and heme trafficking, *Am. J. Hematol.*, 2020, 95(9), 1085–1098.
71. T. Mourer, A. Brault and S. Labbé, Heme acquisition by Shu1 requires Nbr1 and proteins of the ESCRT complex in *Schizosaccharomyces pombe*, *Mol. Microbiol.*, 2019, 112(5), 1499–1518.
72. J. Y. Kim and M. Yenari, Heat shock proteins and the stress response, In: L. R. Caplan, J. Biller, M. C. Leary, E. H. Lo, A. J. Thomas, M. Yenari J. H. Zhang (eds), *Primer on Cerebrovascular Diseases*, Elsevier, 2017, 273–275.
73. G. Liu, D. Sil, N. Maio, W. - H. Tong, J. M. Bollinger, C. Krebs and T. A. Rouault, Heme biosynthesis depends on previously unrecognized acquisition of iron-sulfur cofactors in human amino-levulinic acid dehydratase, *Nat. Commun.*, 2020, 11(1), 6310.
74. H. Zheng, J. Li and C. Feng, Heat shock protein 90 enhances the electron transfer between the FMN and heme cofactors in neuronal nitric oxide synthase, *FEBS Lett.*, 2020, 594(17), 2904–2913.
75. A. Ghosh, G. Garee, E. A. Sweeny, Y. Nakamura and D. J. Stuehr, Hsp90 chaperones hemoglobin maturation in erythroid and nonerythroid cells, *Proc. Natl. Acad. Sci.*, 2018, 115(6), E1117—E1126.
76. A. Ghosh, M. Chawla-Sarkar and D. J. Stuehr, Hsp90 interacts with inducible NO synthase client protein in its heme-free state and then drives heme insertion by an ATP-dependent process, *FASEB J. Off. Publ. Fed. Am. Soc. Exp. Biol.*, 2011, 25(6), 2049–2060.
77. Y. Dai, S. Schlanger, M. M. Haque, S. Misra and D. J. Stuehr, Heat shock protein 90 regulates soluble guanylyl cyclase maturation by a dual mechanism, *J. Biol. Chem.*, 2019, 294(35), 12880–12891.
78. X. Chen, W. Lu, M. - Y. Tsai, S. Jin and P. G. Wolynes, Exploring the folding energy landscapes of heme proteins using a hybrid AWSEM-heme model, *J. Biol. Phys.*, 2022, 48(1), 37–53.
79. L. R. C. Vasconcellos, F. F. Dutra, M. S. Siqueira, H. A. Paula-Neto, J. Dahan, E. Kiarely, L. A. M. Carneiro, M. T. Bozza and L. H. Travassos, Protein aggregation as a cellular response to oxidative stress induced by heme and iron, *Proc. Natl. Acad. Sci.*, 2016, 113(47).

80. A. Rajagopal, A. U. Rao, J. Amigo, M. Tian, S. K. Upadhyay, C. Hall, S. Uhm, M. K. Mathew, M. D. Fleming, B. H. Paw, M. Krause and I. Hamza, Haem homeostasis is regulated by the conserved and concerted functions of HRG-1 proteins, *Nature*, 2008, 453(7198), 1127–1131.
81. J. G. Quigley, Z. Yang, M. T. Worthington, J. D. Phillips, K. M. Sabo, D. E. Sabath, C. L. Berg, S. Sassa, B. L. Wood and J. L. Abkowitz, Identification of a human heme exporter that is essential for erythropoiesis, *Cell*, 2004, 118(6), 757–766.
82. S. P. Duffy, J. Shing, P. Saraon, L. C. Berger, M. V. Eiden, A. Wilde and C. S. Tailor, The Fowler syndrome-associated protein FLVCR2 is an importer of heme, *Mol. Cell. Biol.*, 2010, 30(22), 5318–5324.
83. A. Galmozzi, B. P. Kok, A. S. Kim, J. R. Montenegro-Burke, J. Y. Lee, R. Spreafico, S. Mosure, V. Albert, R. Cintron-Colon, C. Godio, W. R. Webb, B. Conti, L. A. Solt, D. Kojetin, C. G. Parker, J. J. Peluso, J. K. Pru, G. Siuzdak, B. F. Cravatt and E. Saez, PGRMC2 is an intracellular haem chaperone critical for adipocyte function. *Nature*, 2019, 576(7785), 138–142.
84. C. Fufezan, J. Zhang and M. R. Gunner, Ligand preference and orientation in b- and c-type heme-binding proteins, *Proteins Struct. Funct. Bioinf.*, 2008, 73(3), 690–704.
85. L. J. Smith, A. Kahraman and J. M. Thornton, Heme proteins—diversity in structural characteristics, function, and folding, *Proteins Struct. Funct. Bioinf.*, 2010, 78(10), 2349–2368.
86. Y. Kabe, T. Nakane, I. Koike, T. Yamamoto, Y. Sugiura, E. Harada, K. Sugase, T. Shimamura, M. Ohmura, K. Muraoka, A. Yamamoto, T. Uchida, S. Iwata, Y. Yamaguchi, E. Krayukhina, M. Noda, H. Handa, K. Ishimori, S. Uchiyama, T. Kobayashi and M. Suematsu, Haem-dependent dimerization of PGRMC1/Sigma-2 receptor facilitates cancer proliferation and chemoresistance, *Nat. Commun.*, 2016, 7(1), 11030.
87. R. A. Homan, A. M. Jadhav, L. P. Conway and C. G. Parker, A chemical proteomic map of heme-protein interactions, *J. Am. Chem. Soc.*, 2022, 144(33), 15013–15019.
88. A. R. Reddi, C. J. Reedy, S. Mui and B. R. Gibney, Thermodynamic investigation into the mechanisms of proton-coupled electron transfer events in heme protein maquettes, *Biochemistry*, 2007, 46(1), 291–305.
89. C. J. Reedy and B. R. Gibney, Heme protein assemblies, *Chem. Rev.*, 2004, 104(2), 617–650.
90. C. J. Reedy, M. M. Elvekrog and B. R. Gibney, Development of a heme protein structure-electrochemical function database, *Nucleic Acids Res.*, 2008, 36(Database), D307–D313.
91. L. Zhang and L. Guarente, Heme binds to a short sequence that serves a regulatory function in diverse proteins, *EMBO J.*, 1995, 14(2), 313–320.
92. T. Kühl, N. Sahoo, M. Nikolajski, B. Schlott, S. H. Heinemann and D. Imhof, Determination of hemin-binding characteristics of proteins by a combinatorial peptide library approach, *ChemBioChem*, 2011, 12(18), 2846–2855.
93. T. Kühl, A. Wißbrock, N. Goradia, N. Sahoo, K. Galler, U. Neugebauer, J. Popp, S. H. Heinemann, O. Ohlenschläger and D. Imhof, Analysis of Fe(III) heme binding to cysteine-containing heme-regulatory motifs in proteins, *ACS Chem. Biol.*, 2013, 8(8), 1785–1793.
94. E. Schubert, N. Florin, F. Duthie, H. Henning Brewitz, T. Kühl, D. Imhof, G. Hagelueken and O. Schiemann, Spectroscopic studies on peptides and proteins with cysteine-containing heme regulatory motifs (HRM), *J. Inorg. Biochem.*, 2015, 148, 49–56.
95. B. F. Syllwasschy, M. S. Beck, I. Družeta, M. - T. Hopp, A. Ramoji, U. Neugebauer, S. Nozinovic, D. Menche, D. Willbold, O. Ohlenschläger, T. Kühla and D. Imhofa, High-affinity binding and catalytic activity of His/Tyr-based sequences: Extending heme-regulatory motifs beyond CP, *Biochim. Biophys. Acta General Subjects*, 2020, 1864(7), 129603.
96. A. A. Paul George, M. Lacerda, B. F. Syllwasschy, M. - T. Hopp, A. Wißbrock and D. Imhof, HeMoQuest: a webserver for qualitative prediction of transient heme binding to protein motifs, *BMC Bioinf.*, 2020, 21(1), 124.